Analyst

RSC Publishing

PAPER

View Article Online
View Journal | View Issue

Cite this: *Analyst*, 2013, **138**, 1459

A novel platform for enhanced biosensing based on the synergy effects of electrospun polymer nanofibers and graphene oxides†

Xiaofang Su,[ab] Jun Ren,*[a] Xianwei Meng,*[a] Xiangling Ren[a] and Fangqiong Tang*[a]

Received 11th November 2012
Accepted 17th December 2012

DOI: 10.1039/c2an36663k

www.rsc.org/analyst

A novel biosensing platform was developed by combining the advantages of electrospun poly(vinyl alcohol) (PVA)/chitosan nanofibers and graphene oxides (GO). Glucose oxidase (GOD) was employed as a model enzyme. By co-electrospinning the solution of PVA, chitosan, GOD and GO, the PVA/chitosan/GOD/GO nanofibers were directly modified on the platinum (Pt) electrode. The UV-vis spectra and the FTIR spectra were used to characterize the GO nanosheets. The morphologies of fabricated electrospun nanofibers were characterized by high resolution scanning electron microscopy. After a thin layer of nafion was modified on the surface of matrix, the as-prepared electrode was used to detect glucose. The electrode exhibited great advantages in high sensitivity, low detection limit and wide linear range. In the meantime, the electrode showed good stability, acceptable reproducibility, and excellent anti-interference capability for ascorbic acid, uric acid, lactose and sucrose. Moreover, the novel biosensor was successfully applied for the glucose determination in human serum samples. The mechanism of efficient biosensing of the nafion/PVA/chitosan/GOD/GO/Pt electrode was analyzed in detail and the results show that it can be due to the synergy effects of electrospun nanofibers and GO nanosheets.

1 Introduction

In recent years, there has been growing research interest in the tailoring of enzyme immobilization membranes for fully validated biosensors fit for application.[1–4] Electrospinning seems to be the most facile and effective technique to tune the composition, architectures and patterns of the biosensing membrane.[5–7] The qualification of electrospun nanofibers as an ideal platform for highly sensitive biosensing is attributed to: (1) the three-dimensional nanofiber structures endow them with large active surface areas,[8–10] high enzyme loading capacities,[9,10] and a low hindrance for mass transfer,[8–10] and (2) the simple, durable, and adjustable process provides both stability and reproducibility of the biosensor.[11] Therefore, many excellent biosensors have been successfully constructed based on different kinds of electrospun nanofibers. For example, electrospun SnO_2 nanofibers, polyaniline nanofibers, and Mn_2O_3–Ag nanofibers have been applied for the sensitive biosensing of ethanal,[12] cholesterol,[13] and glucose.[14]

Among the various techniques loading enzymes in the nanofibers, the direct co-electrospinning of enzymes and other components (organic or inorganic materials) is the simplest method.[10,15] To achieve the process, the polymers are required to be hydrophilic so that they can form homogeneous solution with the enzymes. Meanwhile, the hydrophilic polymers usually have excellent biocompatibility, which can preserve the enzyme-activity to a large extent.[16] By direct co-electrospinning, the enzyme molecules are immobilized on and within the nanofibers. However, enzymes, which reside on the surface of electrospun nanofibers, tend to leach out from the surface when the nanofibrous membrane is placed in a solution.[17] The accessibility of the substrate to enzymes is inhibited when the enzymes are confined inside the electrospun nanofibers.[18] Therefore, it is essential to have an additional nanomaterial that will bind the enzyme in the nanofibers to minimize the leaching of the enzyme, and provide a good access of substrate to enzyme. In fact, a few attempts have been made to meet the above-mentioned needs for hydrophobic polymer nanofibers. For example, multiwall carbon nanotubes have been dispersed in electrospun polymethylmethacrylate nanofibers, which not only realize the effective immobilization of enzymes in nanofibers but also promote the current response to glucose.[19] But, such efforts are very scarce for electrospun hydrophilic nanofibers.

Among the various nanomaterials, graphene has exhibited unique advantages as biosensing platform, including high surface area, excellent electric conductivity, strong mechanical strength, ease of functionalization and good biocompatibility.[20–25] In addition, graphene oxides (GO) can be uniformly

[a]*Laboratory of Controllable Preparation and Application of Nanomaterials, Technical Institute of Physics and Chemistry, Chinese Academy of Sciences, Beijing 100190, China. E-mail: tangfq@mail.ipc.ac.cn; Fax: +86 10 62554670; Tel: +86 10 82543521*

[b]*University of Chinese Academy of Sciences, Beijing, China*

† Electronic supplementary information (ESI) available: Supporting tables and figures. See DOI: 10.1039/c2an36663k

dispersed in water because of their rich hydroxyl groups and carboxyl groups.[26] Graphene oxides can bind enzyme molecules through electrostatic interactions,[27] thus avoiding the leaching of enzymes from modified electrodes. The graphene-based biosensors have been successfully used for the detection of nitric oxide,[28] dopamine,[29] maltose and glucose.[30] To our knowledge, there have been no reports of biosensors based on the combination of graphene oxides and electrospun nanofibers. So it is quite significant to introduce graphene oxides into electrospun hydrophilic nanofibers to construct a novel and facile enzyme-based biosensing membrane.

Herein, a novel and facile biosensing platform combining the benefits of electrospun hydrophilic poly(vinyl alcohol) (PVA)/chitosan nanofibers and GO was constructed *via* one step co-electrospinning. Glucose oxidase (GOD) was employed as a model enzyme for its cost-effectiveness and good stability. The nafion/PVA/chitosan/GOD/GO/Pt electrode exhibited efficient biosensing for glucose. More importantly, the synergy mechanism of electrospun PVA/chitosan nanofibers and GO nanosheets for efficient biosensing was intensively studied for the first time. The novel biosensing matrix composed of PVA/chitosan nanofibers and GO nanosheets has great promise to be extended to determine important bioanalytes.

2 Experimental

2.1 Materials

Polyvinyl alcohol (PVA, $M_w = 95\,000$) was purchased from J&K Scientific Ltd. Chitosan was from Guo Yao Chemical Reagent Company. Glucose oxidase was extracted from *Aspergillus niger* (Sigma company, 17.3 U mg^{-1}). β-D-Glucose was purchased from Sigma and nafion was from DuPont company. Choline oxidase was extracted from *Alcaligenes* species (Sigma company, 11 U mg^{-1}). Choline chloride were purchased from Sigma. Glutaraldehyde (GA) and potassium ferricyanide were purchased from the Beijing Chemical Plant. Phosphate buffers containing 0.1 M KCl consisted of KH_2PO_4 and Na_2HPO_4 (0.2 M, pH 6.8). Graphene oxides were prepared according to the previous report.[31] All reagents were used without further purification and prepared with distilled water.

2.2 Electrospinning

PVA/chitosan/GO/GOD nanofibers were prepared by electrospinning. Firstly, PVA–chitosan mixed solutions were prepared. 20% PVA solutions and 4% chitosan solutions (2% acetic acid was the solvent) were mixed together under magnetic stirring overnight with a mass ratio of PVA–chitosan equivalent to 2 : 1 to achieve a homogeneous solution. Secondly, glucose oxidase solutions, GO solutions and glutaraldehyde solutions were successively added into the above PVA–chitosan mixed solutions under magnetic stirring for 10 min. Thirdly, electrospinning was carried out. The as-prepared mixed solutions were loaded into a 5 mL syringe with a needle having an inner diameter of 0.8 mm and connected to a high-voltage power supply. An electric potential of 15 kV was applied between the orifice and the collection at a distance of 15 cm. Under the above fixed electrospinning conditions, a polymer jet was formed. Then the nanofiber mats were formed on the surface of collection.

2.3 Preparation of enzyme electrodes

The Pt electrode was sonicated in water, ethanol and acetone for 10 min, respectively, followed by drying at room temperature. The PVA/chitosan/GOD/GO nanofibers were directly electrospun onto the surface of Pt electrode. After electrospinning, the electrode modified with electrospun PVA/chitosan/GOD/GO nanofibers was then placed in glutaraldehyde vapor for crosslinking to form water-insoluble nanofibers. The as-prepared enzyme electrode was defined as the PVA/chitosan/GOD/GO/Pt electrode. For comparison, the PVA/chitosan/GOD/Pt electrode was fabricated under the same conditions. In addition, the casting-PVA/chitosan/GOD/GO/Pt electrode and the casting-PVA/chitosan/GOD/Pt electrode were constructed by the traditional casting method in which the amount of sensing membrane was the same as electrospun nanofibrous membrane by controlling the weight. To meet the anti-interference need in glucose determination, a thin layer of nafion was modified onto the above prepared electrodes by dipping the electrodes into 2.5% nafion solutions for 10 min and then drying at room temperature. So the nafion/PVA/chitosan/GOD/GO/Pt electrode, the nafion/PVA/chitosan/GOD/Pt electrode, the casting-nafion/PVA/chitosan/GOD/GO/Pt electrode, and the casting-nafion/PVA/chitosan/GOD/Pt electrode were obtained. These electrodes were stored at 4 °C before measurement.

2.4 Apparatus and measurements

UV-vis absorbance spectra were recorded using a JASCO V-570 spectrophotometer. Fourier transform infrared (FTIR) spectra was obtained with an Excalibur 3100 spectrometer. The fluorescence measurements were performed using a Cary Eclipse fluorescence spectrophotometer (Varian, Inc.). High resolution scanning electron microscopy (HRSEM) was performed with a Hitachi S-4800 scanning electron microscope. Transmission electron microscope (TEM) was obtained with a JEM-2100 electron microscope operating at 200 KV.

Cyclic voltammetry was performed using a CHI 604B electrochemical workstation (Shang Hai Chen Hua company) in 5 mM $K_3Fe(CN)_6$ containing 0.1 M KCl. A conventional three-electrode system was used throughout the electrochemical experiment at room temperature with a modified electrode as working electrode, a bare Pt electrode as auxiliary electrode, and a saturated calomel electrode (SCE) as reference electrode.

The current response was tested using a three-electrode cell consisting of a modified electrode as working electrode, a bare Pt electrode as auxiliary electrode and a reference electrode of Ag/AgCl. The measurements were conducted at 37 °C. A fixed potential of 0.4 V was applied to this electronic cell. Firstly, the three-electrode cell was put into phosphate solution. When background current reached a constant value, different concentrations of β-D-glucose solution were added. Then response currents were noted down, and background currents were deducted. At last, the correlation between the current response and the concentrations of glucose solution was obtained.

3 Results and discussion

3.1 The characterization of GO, PVA/chitosan/GOD nanofibers, and PVA/chitosan/GOD/GO nanofibers

The characterization of GO was performed by UV-vis spectra and FTIR spectra. The UV-vis spectra of graphene oxides (in Fig. 1(A)) in water show an absorption peak at 230 nm, which is in accord with the previous report of Li's group.[32] The FTIR spectra of graphene oxides in Fig. 1(B) show the absorption peaks at 3400, 1631, 1400, 1056 cm^{-1}, which can be attributed to the characteristic peaks of O–H, C=C, C=C, and C–O in graphene, respectively.[33,34] The graphene oxide is the flake-like shape (Fig. S1(A)†). A selected-area electron diffraction of graphene oxides can yield a double six-spot-ring pattern from a graphene oxide sheet (the inset of Fig. S1(A)†). In addition, GO nanosheets exhibit some wrinkled structure (Fig. S1(B and C)†), and this wrinkled nature of GO nanosheets is highly beneficial in maintaining a high surface area on the electrode since the sheets cannot readily collapse back to a graphitic structure.[35]

The morphologies of PVA/chitosan/GOD nanofibers and PVA/chitosan/GOD/GO nanofibers were characterized by HRSEM. Fig. 1(C) shows the HRSEM image of PVA/chitosan/GOD nanofibers, indicating a relatively homogeneous fibrous structure. In comparison, the flake structure emerges in the PVA/chitosan/GOD/GO nanofibrous matrix, as shown in Fig. 1(D). These flake structures may result from the graphene oxide nanosheets loaded in PVA/chitosan nanofibers through electrospinning (Fig. S1(E)†). In addition, the above-mentioned wrinkled state of graphene oxides may be advantageous to their distribution in nanofibers in the process of electrospinning (Fig. S1(F)†). The successful loading of GO in nanofibers may play a crucial role in the conductivity of matrix, the immobilization of enzyme molecules and the access of enzymes to the substrate.

3.2 The evaluation of the electrochemical performance of different electrodes

The cyclic voltammetric (CV) experiments in 5.0 mM potassium ferricyanide solution were employed to evaluate the electrochemical performance of different electrodes. As shown in Fig. 2(A), the well-defined oxidation and reduction peaks caused by the Fe^{3+}–Fe^{2+} redox couples were noticed in forward and reverse scan for the bare Pt electrode (curve a). When the enzyme membranes composed of different components were modified onto Pt electrode, the distinct electrochemical properties of modified electrodes were observed. In brief, the electrospun nanofibrous membrane-modified electrodes (the PVA/chitosan/GOD/GO/Pt, curve b; the PVA/chitosan/GOD/Pt, curve c) have higher oxidation and reduction peak currents than the casting membrane-modified electrodes (the casting-PVA/chitosan/GOD/GO/Pt, curve d; the casting-PVA/chitosan/GOD/Pt, curve e), which indicates the unique advantages of electrospun nanofibers as sensing matrix. The large surface to volume area and high porosity of electrospun nanofibers can increase the electro-active area of electrodes and reduce the diffusion resistance of substrates obviously. Meanwhile, the peak currents of GO-modified electrodes are higher than those of no GO modified-electrodes of the same style: the PVA/chitosan/GOD/GO/Pt (curve b) > the PVA/chitosan/GOD/Pt (curve c), the casting-PVA/chitosan/GOD/GO/Pt (curve d) > the casting-PVA/chitosan/GOD/Pt (curve e). This demonstrates the excellent electrochemical properties of GO, such as excellent electrical conductivity and large surface area, which can improve the conductivity and active area of nanofibrous/casting membrane. More importantly, the PVA/chitosan/GOD/GO/Pt electrode composed of electrospun nanofibers and GO exhibits optimal oxidation and reduction capability towards electro-active species, even compared with the bare Pt electrode. The excellent electrochemical properties of PVA/chitosan/GOD/GO/Pt electrode may be due to the synergy effects of PVA/chitosan nanofibers and GO nanosheets. Fig. 2(B) shows the effect of the scan rate on the peak current of the PVA/chitosan/GOD/GO/Pt electrode, and Fig. 2(C) is the plots of peak current *versus* the square root of

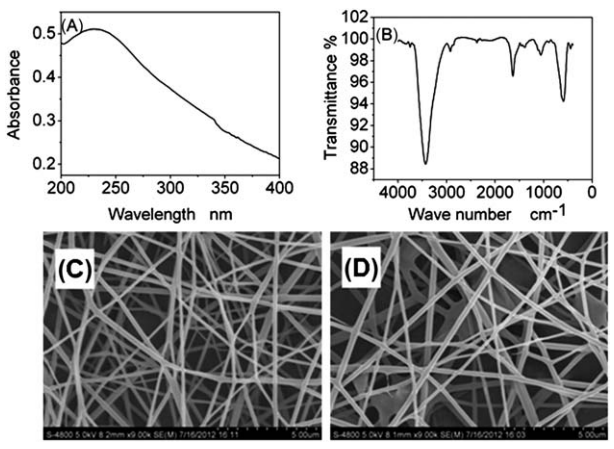

Fig. 1 (A) The UV-vis spectra of graphene oxides in water. (B) The FTIR spectra of graphene oxides. (C) The HRSEM images of PVA/chitosan/GOD nanofibers. (D) The HRSEM images of PVA/chitosan/GOD/GO nanofibers.

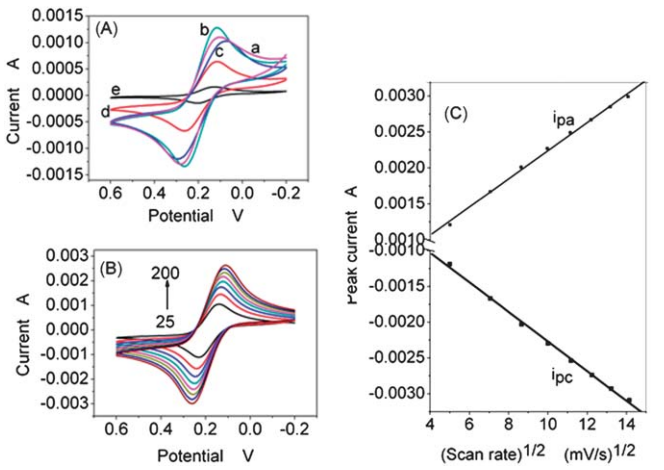

Fig. 2 (A) The cyclic voltammograms of different electrodes in 5.0 mM potassium ferricyanide solution containing 0.1 M KCl: (a) the bare Pt, (b) the PVA/chitosan/GOD/GO/Pt; (c) the PVA/chitosan/GOD/Pt, (d) the casting-PVA/chitosan/GOD/GO/Pt, (e) the casting-PVA/chitosan/GOD/Pt. (B) The effect of scan rate on the cyclic voltammograms of the PVA/chitosan/GOD/GO/Pt. (C) The plots of peak current *versus* the square root of scan rate.

scan rate. It can be seen that the oxidation and reduction peak currents increase linearly with the square root of the scan rate, indicating the reaction is controlled by a semi-infinite linear diffusion.[36] All of the above results suggest that the PVA/chitosan/GOD/GO/Pt electrode is more beneficial for the electron transfer, resulting from the combination of GO nanosheets and PVA/chitosan/GOD nanofibers.

3.3 The optimization of nafion/PVA/chitosan/GOD/GO/Pt electrode

To optimize the performance of the as-prepared electrode, the response currents for 2.5 mM glucose solution were noted down under different preparation and measurement conditions.

Fig. 3(A) shows the influence of GO concentration on the response current of enzyme electrode. It can be seen that when GO are loaded in the enzyme electrode with concentration from 20–180 μg g^{-1}, the overall response currents are increased to various degrees. It indicates that GO plays an important role in the improvement of glucose response ability of enzyme electrode. The highest response current is observed at the GO concentration of 100 μg g^{-1}. With higher GO concentration, the aggregation of GO in the electrospun solution occurs, which decreases the electrospinning property of electrospun solution and may lead to the activity loss of enzyme, thus decreasing the response current of enzyme electrode. So 100 μg g^{-1} is chosen as the optimum concentration of GO, and this concentration is fixed in Fig. 3(B)–(D).

Fig. 3(B) shows the response curve of enzyme electrodes with different GOD concentrations. With the increase of GOD concentration, the response current increases gradually. However, when the enzyme concentration is higher than 3.6 mg g^{-1}, the response current tends to be saturated. Further increment of enzyme concentration would be a waste of this expensive reagent, so in the following experiments the enzyme concentration is set as 3.6 mg g^{-1}.

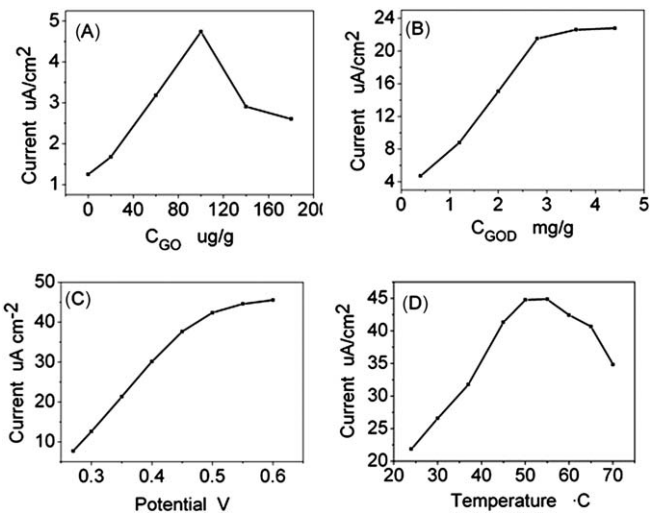

Fig. 3 The optimization of the nafion/PVA/chitosan/GOD/GO/Pt electrode: The current response of the enzyme electrode in 2.5 mM glucose (A) with varying GO concentration, (B) with varying enzyme concentration, (C) with varying working potential, (D) with varying temperature.

The choice of working potential is necessary to achieve the highest sensitivity and avoid the electrochemical interfering species. Fig. 3(C) shows the effect of working potential on the response current of enzyme electrode from 0.27 V to 0.60 V. The oxidation current for glucose of enzyme electrode increases with increasing the potential obviously. However, the higher background current and longer balance time are observed when the potential is over 0.40 V, which is disadvantageous for sensitive and rapid determination. Meanwhile, the co-existing electrochemical interfering species in solution tend to be oxidized more easily at higher working potential, which would make it difficult to detect glucose very accurately. Considering the above factors, 0.40 V is selected for all the subsequent amperometric detections.

Temperature has a great effect on the enzyme–catalysis reaction kinetics and enzyme activity. So choosing an appropriate measurement temperature plays a very important role in the highly sensitive determination of biosensor. The glucose response curve of enzyme electrode at different temperatures is shown in Fig. 3(D). It shows that the response current is enhanced with increasing temperature from 24 to 55 °C. It is due to that the rate constant of enzyme–catalysis reaction can be increased dramatically with the temperature increase. However, the response current decreases when the temperature is higher than 55 °C, because extra-high temperature can lead to the denaturation of enzyme and then the loss of enzyme activity. In addition, the as-prepared biosensor may be applied in some special conditions, such as the analysis for the human serum sample. In order to keep consistent with the temperature of human body, 37 °C is selected for this work.

3.4 The comparison of glucose determination of different electrodes

Under the optimum conditions, the nafion/PVA/chitosan/GOD/GO/Pt electrode was used for the glucose amperometric detection. The results obtained were compared with the nafion/PVA/chitosan/GOD/Pt electrode, the casting-nafion/PVA/chitosan/GOD/GO/Pt electrode, and the casting-nafion/PVA/chitosan/GOD/Pt electrode. As shown in Fig. 4(A), the response current of the electrospun nanofibrous membrane-modified electrodes are superior to the casting ones: the nafion/PVA/chitosan/GOD/GO/Pt (curve a) > the casting-nafion/PVA/chitosan/GOD/GO/Pt (curve b), the nafion/PVA/chitosan/GOD/Pt (curve c) > the casting-nafion/PVA/chitosan/GOD/Pt (curve d). This demonstrates the benefits of electrospun nanofibers as biosensing platform. In the meantime, the response currents for glucose of the GO-modified electrodes (the nafion/PVA/chitosan/GOD/GO/Pt, curve a; the casting-nafion/PVA/chitosan/GOD/GO/Pt, curve b) are higher than those of the no GO-modified electrodes (the nafion/PVA/chitosan/GOD/Pt, curve c; the casting-nafion/PVA/chitosan/GOD/Pt, curve d), which reflects the unique advantages of GO for glucose amperometric determination. In particular, by the combination and synergy of electrospun nanofibers and GO, the as-prepared nafion/PVA/chitosan/GOD/GO/Pt electrode shows the highest response currents for glucose, compared to other electrodes. For example, in 1 mM

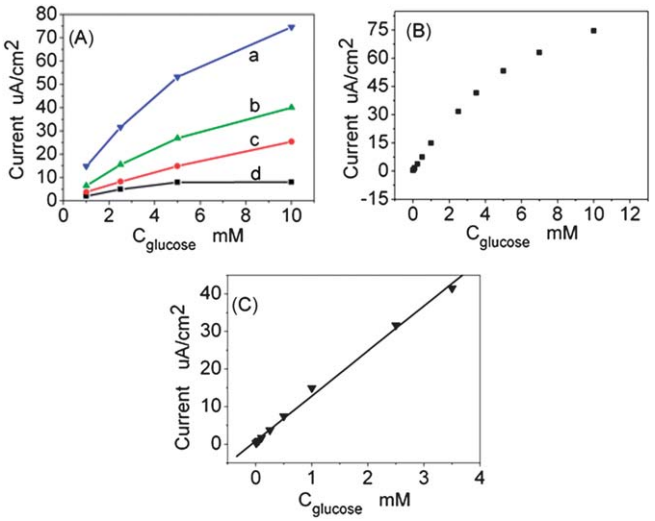

Fig. 4 (A) The comparison of current response to glucose of different electrodes: (a) the nafion/PVA/chitosan/GOD/GO/Pt, (b) the casting-nafion/PVA/chitosan/GOD/GO/Pt, (c) the nafion/PVA/chitosan/GOD/Pt, (d) the casting-nafion/PVA/chitosan/GOD/Pt. (B) The current response of the nafion/PVA/chitosan/GOD/GO/Pt at different glucose concentrations. (C) The calibration curve for glucose of the nafion/PVA/chitosan/GOD/GO/Pt electrode.

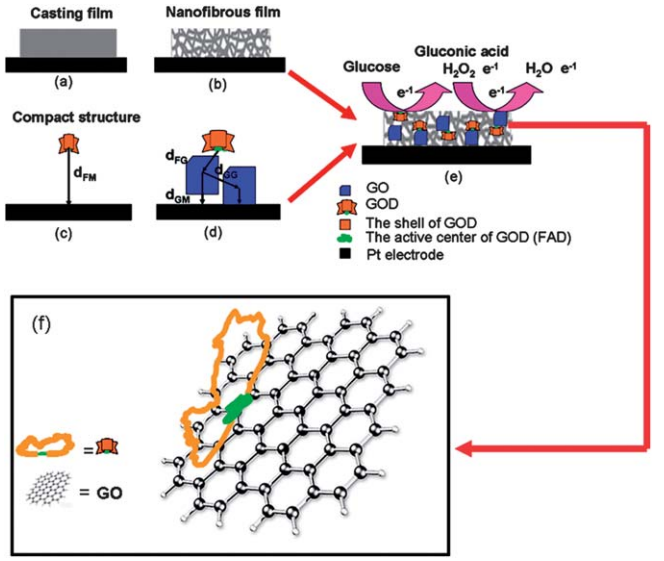

Fig. 5 The mechanism presentation of efficient biosensing in nafion/PVA/chitosan/GOD/GO/Pt electrode: (a) the structure of casting film, (b) the structure of electrospun nanofibrous film, (c) the compact enzyme structure in electrode without GO, (d) the unfolding enzyme structure in electrode with GO, (e) the efficient biosensing is realized *via* the synergy effects of electrospun nanofibers and GO, (f) the schematic picture of the interaction between GOD and GO.

glucose solution, the response current of the nafion/PVA/chitosan/GOD/GO/Pt electrode is 7.4 times higher than that of the casting-nafion/PVA/chitosan/GOD/Pt electrode. Fig. 4(B) shows the current response of the nafion/PVA/chitosan/GOD/GO/Pt at different glucose concentrations. The calibration curve is shown in Fig. 4(C), which demonstrates a high sensitivity of 11.98 μA cm^{-1} mM^{-1}, a wide linear range of 5 μM–3.5 mM, and a low detection limit of 5 μM. We also compare the performance of the nafion/PVA/chitosan/GOD/GO/Pt electrode with that of some former work, and the results are listed in Table S1.† It indicates that the as-prepared biosensor exhibits great advantages in sensitivity, detection limit and linear range, when compared to other biosensors with similar electrode construction styles.

3.5 The possible mechanism of efficient biosensing of nafion/PVA/chitosan/GOD/GO/Pt electrode

The biosensing efficiency of enzyme electrode is strongly dependent on the diffusion of substrates in sensing membrane; the properties of enzyme, including the active center accessibility and the binding efficiency; the conductivity and active surface area of biosensing matrix; the ability of the modified electrode that converts the substrate/intermediate to product; the microenvironment of electrode *etc.*

As has been discussed in Fig. 2(A) and 4(A), the electrospun nanofibrous membrane exhibited more excellent properties for biosensing than the casting membrane, which may originate from their intrinsic structures. Fig. 5(a) shows the dense structure of the casting membrane, which would not be conductive to the diffusion of substrates. In contrast, the electrospun nanofibrous membrane has very high porosity and large surface area, as is shown in Fig. 5(b). It can significantly reduce the diffusion resistance of substrates and then increase the response to electro-active species of modified electrodes. Therefore, the more rapid diffusion of substrates in electrospun nanofibers can be beneficial for the efficient biosensing of the as-prepared electrode.

GOD is an enzyme with the flavin adenine dinucleotide (FAD) as its active center, which is usually deeply embedded in the interior of the protein shell, as can be seen in Fig. 5(c). The relatively large distance between FAD and metal electrode surface (d_{FM}) would make it very difficult to transfer electrons directly. On the contrary, when the rigid protein shell is unfolded and then the active center of enzyme (FAD) is exposed, the rate coefficient of electron transfer between the donator and acceptor may increase exponentially.[37] The fluorescence spectroscopy is a powerful technique to monitor unfolding transitions and to characterize properties of the unfolded state of protein. The fluorescence intensity will decrease and the maximum wavelength will have a red shift, accompanied with the unfolding process of protein in an aqueous solution.[38] The above mentioned phenomenon of protein unfolding indeed occurs in our research, as is shown in Fig. 6(A). It indicates that the protein shell is unfolded and the active center (FAD) is exposed to some extent with the induction effect of GO, which is described vividly in Fig. 5(d) and (f). In addition, the distance between FAD and mental electrode is reduced obviously with GO nanosheets as electron-conducting pathways. The results are in conformity with the former reports about the direct electron transfer between enzyme and electrode *via* carbon nanotube[39] and gold nanoparticles.[37]

In the meantime, the loading of GO, with excellent conductivity and large surface area, can improve the conductive property of polymer matrix and increase the electro-active area of the

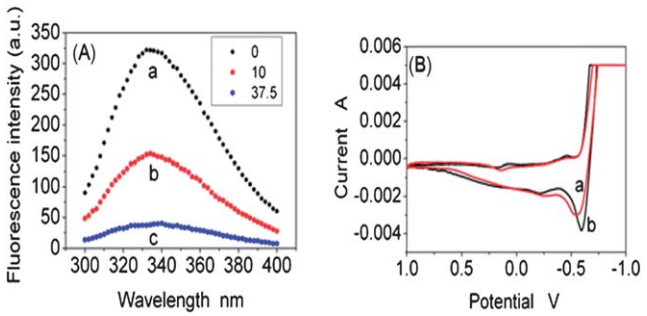

Fig. 6 (A) The fluorescence spectrum of GOD in water at different GO concentration: (a) 0, (b) 10 μg mL^{-1}, (c) 37.5 μg mL^{-1}. (B) The cyclic voltammetric curves of different electrodes in 5 mM glucose solution: (a) the nafion/PVA/chitosan/GOD/Pt electrode, (b) the nafion/PVA/chitosan/GOD/GO/Pt electrode.

sensing membrane combined with the electrospun nanofibers. These discussions can be confirmed by the results in Fig. 2. On the other hand, GO can bind the enzyme molecules in nanofibers more firmly *via* electrostatic interactions, which also benefits the current response of enzyme electrodes.

In the enzyme–catalysis reaction, GOD can selectively catalyze the oxidation of glucose in the presence of oxygen to form H_2O_2, which can be electrochemically detected.[40] The electro-oxidation capacity for the intermediate H_2O_2 also plays a vital part in the response performance of enzyme electrode. Fig. 6(B) compares the CV curves of the nafion/PVA/chitosan/GOD/Pt electrode and the nafion/PVA/chitosan/GOD/GO/Pt electrode in 5 mM glucose solution. It can be seen that the oxidation peak of H_2O_2 can be observed at −0.56 V and −0.60 V for the PVA/chitosan/GOD/Pt electrode and the PVA/chitosan/GOD/GO/Pt electrode respectively. Moreover, the H_2O_2 oxidation peak current of the nafion/PVA/chitosan/GOD/GO/Pt electrode is dramatically increased over that of the nafion/PVA/chitosan/GOD/Pt electrode. The better electro-oxidation performance for H_2O_2 of the nafion/PVA/chitosan/GOD/GO/Pt electrode may be attributed to the high density of edge-plane-like defective sites on GO, which may provide many active sites for electron transfer to electro-active species.[29] Based on the above results, more sensitive determination for glucose may be realized for the GO-modified electrodes, which can be confirmed by the results in Fig. 4(A).

Furthermore, the PVA and chitosan are considered as non-toxic and biocompatible polymers. Meanwhile, recent research[41,42] has proven that GO nanosheets have excellent biocompatibility. Accordingly, in our system, the PVA/chitosan/GO nanofibers would create a quite mild microenvironment for the enzyme immobilization. Although the protein shell is unfolded with the inductive effect of GO, such mild microenvironment from PVA, chitosan and GO will reduce some non-specific enzyme–support interactions and preserve the enzyme activity obviously.

Based on the above discussions, electrospun nanofibers can be greatly conductive to the rapid diffusion of substrates. GO can bring the following influences: (1) the enzyme shell is unfolded and the active center (FAD) is exposed, leading to a dramatic distance decrease of electron transfer; (2) the conductivity of polymer matrix is obviously increased; (3) enzyme molecules can be immobilized more firmly; (4) the electro-catalysis property of H_2O_2 is enhanced to a large degree. In addition, the electrospun nanofibers and GO can increase the electro-active area and benefit for the biocompatibility of composite matrix. As a result, by the combination of electrospun nanofibers and GO, the as-prepared nafion/PVA/chitosan/GOD/GO/Pt electrode can realize the enhanced biosensing for glucose based on the synergy effects of electrospun nanofibers and GO.

3.6 The stability, reproducibility and anti-interference study of nafion/PVA/chitosan/GOD/GO/Pt electrode

We investigated the measurement stability of the nafion/PVA/chitosan/GOD/GO/Pt electrode by amperometric measurements in the presence of 2.5 mM glucose. The current response of enzyme electrode is retained at about 96% of its original response after 50 detections (Fig. S2(A)†). The storage stability was also tested. It reveals that the current response of enzyme electrode maintains 85% after 15 days, and 73% after 30 days, indicating an acceptable storage stability. The good stability of enzyme electrode demonstrates that GOD can maintain good activity in the biocompatible matrix composed of GO nanosheets and PVA/chitosan nanofibers.

The reproducibility of the nafion/PVA/chitosan/GOD/GO/Pt electrode was also evaluated. Under the same fabrication conditions used in this study, six electrodes were prepared for the steady-state current to 2.5 mM glucose at 0.40 V *versus* Ag/AgCl electrode. The results show that the response currents for six individually repetitive tests keep a good consistency with a RSD of 3.5%, indicating a good reproducibility of this procedure.

Anti-interference tests were carried out in 5 mM glucose solutions, followed with additions of 0.1 mM ascorbic acid (AA), 0.1 mM uric acid (UA), 3 mM lactose and 3 mM sucrose. The results demonstrate that the current response of the nafion/PVA/chitosan/GOD/GO/Pt electrode in the solution containing glucose and interfering species, has a good agreement with that in glucose solution (Fig. S2(B)†). The RSD is < 1%. Therefore the nafion/PVA/chitosan/GOD/GO/Pt electrode possesses an excellent anti-interference capability towards AA, UA, lactose and sucrose. It also indicates that the biosensor is of great potential in the analysis of real samples.

3.7 The application of the biosensor to serum samples

The real human serum samples were employed to verify the reliability of the new biosensor in clinical analysis. 400 μL of serum sample was diluted to 4 mL with PBS solution and the response currents were noted down. The concentration of the glucose in serum sample was calculated from the calibration curve. The results are listed in Table 1 and compared with the concentrations of clinical analysis obtained by Automatic Biochemical Analyzer. It shows that the concentrations obtained by the proposed sensor are satisfactory and agree closely with their real values. The results reveal the promise of the new biosensor for glucose determination in clinical analysis.

Table 1 Glucose concentrations in serum samples tested by the proposed method and Automatic Biochemical Analyzer

Serum sample	Clinical assay concentration (mM)	Proposed method concentration (mM)	RSD (%, $n = 3$)
Sample 1	5.54	5.22	−5.8
Sample 2	4.23	4.39	3.6
Sample 3	4.45	4.17	−6.3

3.8 The extended detection for choline chloride of the novel biosensing platform

In order to verify the possible versatile application of the novel biosensing platform composed of PVA/chitosan nanofibers and GO, the choline biosensor was fabricated with the same method as the glucose biosensor, in which GOD was taken place by choline oxidase. The new choline biosensor was applied for the detection of choline chloride (Fig. S3(A)†). The response current increases with increasing choline chloride concentration. The detection limit of choline biosensor is 0.5 mM. In addition, the choline biosensor shows a linear range of 1–8 mM (Fig. S3(B)†). It indicates that the novel biosensing platform composed of PVA/chitosan nanofibers and GO has great promise to immobilize other enzymes and to be extended to determine important bioanalytes.

4 Conclusions

In conclusion, we have developed a novel and enhanced biosensing platform based on electrospun PVA/chitosan nanofibers and graphene oxide nanosheets. The stability, reproducibility, and anti-interference capability were discussed. Furthermore, the new biosensor was successfully applied for the detection of glucose in human serum samples, which indicates the great promise of the new biosensor in clinical analysis. The efficient biosensing for glucose of the fabricated biosensor was achieved *via* the synergy effects of graphene oxides and electrospun polymer nanofibers. The detailed study of graphene-based electrospun nanofibers will open up a new direction of research in sensing, biosensing and clinical diagnostics.

Acknowledgements

We acknowledge financial support from the National Natural Science Foundation of China (Project no. 81171454, 61171049, and 60907042).

Notes and references

1 X. Y. Pang, D. M. He, S. L. Luo and Q. Y. Cai, *Sens. Actuators, B*, 2009, **137**, 134.
2 L. Q. Yang, X. L. Ren, F. Q. Tang and L. Zhang, *Biosens. Bioelectron.*, 2009, **25**, 889.
3 Z. W. Zhao, W. Lei, X. B. Zhang, B. P. Wang and H. L. Jiang, *Sensors*, 2010, **10**, 1216.
4 F. Tasca, R. Ludwig, L. Gorton and R. Antiochia, *Sens. Actuators, B*, 2013, **177**, 64.
5 D. He, B. Hu, Q. F. Yao, K. Wang and S. H. Yu, *ACS Nano*, 2009, **3**(12), 3993.
6 Y. Luo, S. Nartker, H. Miller, D. Hochhalter, M. Wiederoder, S. Wiederoder, E. Setterington, L. T. Drzal and E. C. Alocilja, *Biosens. Bioelectron.*, 2010, **26**, 1612.
7 L. F. Tan, X. L. He, D. Chen, X. L. Wu, H. B. Li, X. L. Ren, X. W. Meng and F. Q. Tang, *J. Biomed. Nanotechnol.*, 2013, **9**, 53.
8 Y. Ding, Y. Wang, B. K. Li and Y. Lei, *Biosens. Bioelectron.*, 2010, **25**, 2009.
9 P. Santhosh, K. M. Manesh, S. H. Lee, S. Uthayakumar, A. I. Gopalan and K. P. Lee, *Analyst*, 2011, **136**, 1557.
10 J. Liu, J. F. Niu, L. F. Yin and F. Jiang, *Analyst*, 2011, **136**, 4802.
11 X. L. He, L. F. Tan, X. L. Wu, C. M. Yan, D. Chen, X. W. Meng and F. Q. Tang, *J. Mater. Chem.*, 2012, **22**, 18471.
12 W. Zheng, X. F. Lu, W. Wang, Z. Y. Li, H. N. Zhang, Y. Wang, Z. J. Wang and C. Wang, *Sens. Actuators, B*, 2009, **142**, 61.
13 Y. J. Shin and J. Kameoka, *J. Ind. Eng. Chem.*, 2012, **18**, 193.
14 S. Huang, Y. Ding, Y. X. liu, L. Su, R. Filosa Jr and Y. Lei, *Electroanalysis*, 2011, **23**(8), 1912.
15 Z. G. Wang, L. S. Wan, Z. M. Liu, X. J. Huang and Z. K. Xu, *J. Mol. Catal. B: Enzym.*, 2009, **56**, 189.
16 A. Hezi-Yamit, C. Sullivan, J. Wong, L. David, M. F. Chen, P. W. Cheng, D. Shumaker, J. N. Wilcox and K. Udipi, *J. Biomed. Mater. Res., Part A*, 2009, **90**, 133.
17 K. M. Manesh, H. T. Kim, P. Santhosh, A. I. Gopalan and K. P. Lee, *Biosens. Bioelectron.*, 2008, **23**, 771.
18 Z. G. Wang, L. S. Wan, Z. M. Liu, X. J. Huang and Z. K. Xu, *J. Mol. Catal. B: Enzym.*, 2009, **56**, 189.
19 Z. G. Wang, Y. Wang, H. Xu, G. Li and Z. K. Xu, *J. Phys. Chem. C*, 2009, **113**, 2955.
20 M. Zhou, Y. M. Zhai and S. J. Dong, *Anal. Chem.*, 2009, **81**, 5603.
21 S. J. Guo, D. Wen, Y. M. Zhai, S. J. Dong and E. Wang, *ACS Nano*, 2010, **4**(7), 3959.
22 J. Li, S. J. Guo, Y. M. Zhai and E. Wang, *Electrochem. Commun.*, 2009, **11**, 1085.
23 C. L. Sun, H. H. Lee, J. M. Yang and C. C. Wu, *Biosens. Bioelectron.*, 2011, **26**, 3450.
24 M. H. Yang, B. G. Choi, H. Park, W. H. Hong, S. Y. Lee and T. J. Park, *Electroanalysis*, 2010, **22**(11), 1223.
25 S. Alwarappan, C. Liu, A. Kumar and C. Z. Li, *J. Phys. Chem. C*, 2010, **114**, 12920.
26 M. J. McAllister, J. L. Li, D. H. Adamson, H. C. Schniepp, A. A. Abdala, J. Liu, M. Herrera-Alonso, D. L. Milius, R. Car, R. K. Prud'homme and I. A. Aksay, *Chem. Mater.*, 2007, **19**, 4396.
27 J. L. Zhang, F. Zhang, H. J. Yang, X. L. Huang, H. Liu, J. Y. Zhang and S. W. Guo, *Langmuir*, 2010, **26**(9), 6083.
28 J. F. Wu, M. Q. Xu and G. C. Zhao, *Electrochem. Commun.*, 2010, **12**, 175.
29 M. Zhou, Y. M. Zhai and S. J. Dong, *Anal. Chem.*, 2009, **81**, 5603.
30 G. H. Zeng, Y. B. Xing, J. Gao, Z. Q. Wang and X. Zhang, *Langmuir*, 2010, **26**(18), 15022.

31 Y. Wang, Y. Huang, Y. Song, X. Y. Zhang, Y. F. Ma, J. J. Liang and Y. S. Chen, *Nano Lett.*, 2009, **9**(1), 220.
32 C. S. Shan, H. F. Yang, D. X. Han, Q. X. Zhang, A. Ivaska and L. Niu, *Biosens. Bioelectron.*, 2010, **25**, 1070.
33 K. P. Liu, J. J. Zhang, G. H. Yang, C. M. Wang and J. J. Zhu, *Electrochem. Commun.*, 2010, **12**, 402.
34 C. S. Shan, H. F. Yang, D. X. Han, Q. X. Zhang, A. Ivaska and L. Niu, *Langmuir*, 2009, **25**(20), 12030.
35 H. Wu, J. Wang, X. H. Kang, C. M. Wang, D. H. Wang, J. Liu, I. A. Aksay and Y. H. Lin, *Talanta*, 2009, **80**, 403.
36 L. H. Tang, Y. Wang, Y. M. Li, H. B. Feng, J. Lu and J. H. Li, *Adv. Funct. Mater.*, 2009, **19**, 2782.
37 S. Sharma, N. Gupta and S. Srivastava, *Biosens. Bioelectron.*, 2012, **37**, 30.
38 A. Kumari, T. Rosenkranz, J. Fitter and A. M. Kayastha, *Protein Pept. Lett.*, 2011, **3**, 253.
39 H. Z. Zhao, J. J. Sun, J. Song and Q. Z. Yang, *Carbon*, 2010, **28**, 1508.
40 W. B. Lu, Y. L. Luo, G. H. Chang and X. P. Sun, *Biosens. Bioelectron.*, 2011, **26**, 4791.
41 H. Q. Chen, M. B. Müller, K. J. Gilmore, G. G. Wallace and D. Li, *Adv. Mater.*, 2008, **20**, 3557.
42 Y. Liu, D. S. Yu, C. Zeng, Z. C. Miao and L. M. Dai, *Langmuir*, 2010, **26**(9), 6158.